Improving the Weldability of Ni-Base Superalloy 713C

HAZ weld cracking is minimized by optimizing welding current and speed as well as energy input

BY A. KOREN, M. ROMAN, I. WEISSHAUS, AND A. KAUFMAN

ABSTRACT. The effect of weld energy input parameters on the cracking tendency of alloy 713C was studied using bead-on-plate plasma arc welding. Quantitative metallographic techniques were used to characterize cracking behavior. Statistical analysis of the data showed that, for the plate dimensions and geometry studied, the tendency to crack decreased with increasing energy input and decreasing welding speed. A mathematical expression which relates the cracking severity to both these parameters was derived empirically from the data.

Improved cracking resistance was attributed to the reduction of the rate of straining imposed on the solidifying weld. The relative importance of welding speed and current is discussed in terms of the rate at which the energy input is transferred to the work-piece.

Introduction

INCO alloy 713C* is a cast Ni-base superalloy widely used for turbine airfoil applications where extreme service conditions prevail. The nominal composition of alloy 713C is given in Table 1.

The high temperature strength of alloy 713C is attributed to a high volume fraction of the γ' phase (approximately 75 wt-%), which is an intermetallic compound consisting mainly of Al, Ti, and Cb combined with Ni. It is common to define γ' strengthened alloys as weldable or nonweldable, depending on the percentage of these elements. In Fig. 1, alloy 713C is seen to be well within the nonweldability range, because of the high content of major γ' forming elements (Al + Ti).

Table 1—Nominal Composition of Alloy 713C, Wt-%

C	0.13	Ti	1.02
Mn	0.2	Al	6.2
S	0.005	B	0.008
Si	0.3	Zr	0.08
Cr	14.2	Fe	0.5
Mo	4.0	Ca	0.3
	Ta + Cb 2.7		

A. KOREN is a research metallurgist, TRW Inc., Cleveland, Ohio; M. ROMAN is a metallurgist, I. WEISSHAUS is chief chemist, Iscar Blades, Israel; A. KAUFMAN is R&D manager, Iscar Ltd., Israel.

Hitherto, the main subjects of research pertaining to weldability of alloy 713C have been concerned with either the cracking mechanism during welding (Ref. 1) or with correlating the cracking phenomenon to minor elements (Ref. 1,2) (e.g., Al, C). However, in the present work, we sought a rather simple technological solution to the weld cracking problem of alloy 713C, for which the alloy's chemistry was not regarded as a variable. Also, major changes in the process, such as argon tent and preheating (Ref. 3), were not considered.

It was assumed that there should be an optimal set of welding parameters at which cracking would be minimized within these constraints. Consequently, an experiment was designed to study the effect of weld energy input and its variables, i.e., weld current and speed on the tendency to crack.

Welding Experiments

Bead-on-plate welding experiments were carried out on cast plates of alloy 713C, one of which is shown in Fig. 2 in the as-welded condition. The cast plates, each 65 × 35 × 6 mm (2.56 × 1.38 × 0.236 in.) in size, were stress relieved in hydrogen atmosphere and x-ray inspected prior to welding experiments, i.e., processed in the same manner as the cast hardware.

The equipment used and the experimental procedure were described elsewhere (Ref. 4) and are summarized in Table 2. After welding, the plates were allowed to cool in still air; the welded side was then very carefully ground flat so as to minimize residual grinding stresses. Polishing was continued manually on abrasive paper and completed electrolytically to remove any possible preparation damages. Figure 3 depicts a fully processed welded plate in which the cracks appear very clearly to facilitate evaluation.

Data Analysis

A quantitative image analyzer ("Quantimet 720") was used to generate the following data:

- Number of cracks in the weld.
- Number of cracks in the heat affected zone (HAZ).
- Distribution of crack lengths in each zone.
- Total number of cracks.†
- Total length of cracks.

Curve fitting statistical analysis was

**Trademark of the INCO family of companies.*

†Total number of cracks = the sum of HAZ cracks, weld cracks and combined cracks.

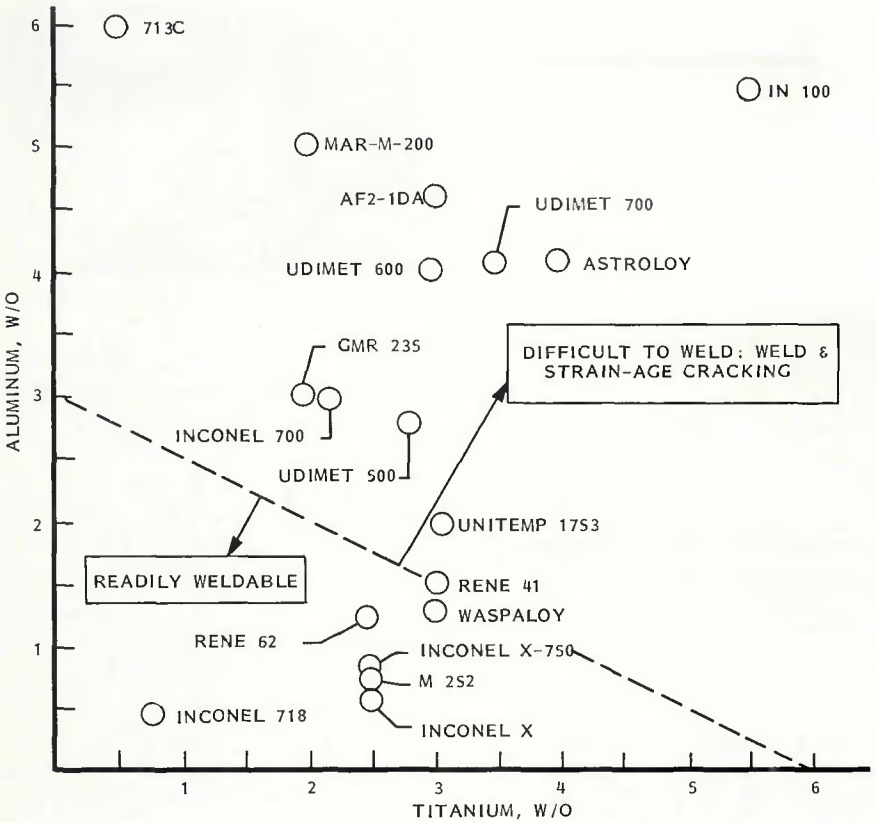

Fig. 1 — Weldability of γ′-strengthened alloys (from M. Prager and C. S. Shira, Welding Research Council Bulletin 128, 1968)

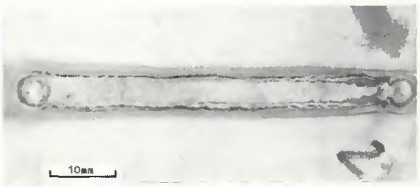

Fig. 2 — Cast IN-713C plate as-welded

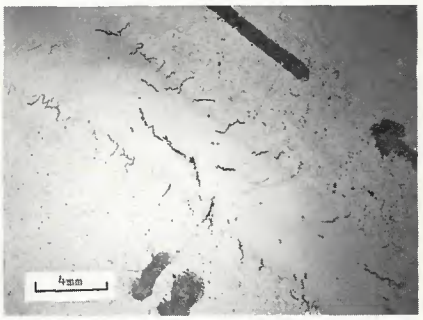

Fig. 3 — Weld cracks clearly visible in an electropolished test plate of IN-713C

conducted by the regression method in order to find the best correlation between any of the above measures of cracking and any of the welding parameters.

Results and Discussion

Of the many possible combinations tested, the correlation between the total number of cracks per cm (Y) and weld energy input (E), emerged to be statistically significant (99% confidence) in the following form:

$$Y = ae^{-bE} \qquad (1)$$

where a and b are constants. A computer plot of this relationship is shown in Fig. 4. Using the double regression method, the energy input components were considered separately. This resulted in the following relationship:

$$Y = 3.4 + 1.73 \ln S - 0.91 \ln I \qquad (2)$$

where I = welding current and S = welding speed.

Equation (2) describes the correlation of the tendency to crack to weld current and weld speed. The coefficients of lnS and lnI, 1.73 and −0.91, respectively, indicate that an increase in the welding speed (while holding the current constant) causes increased cracking while, to a lesser extent, an increase in the welding current at a constant speed reduces this tendency.

From equation (2), it follows that minimum cracking is achievable by aiming at the lowest practical speed and highest practical current while maintaining other variables constant (i.e., voltage, torch angle, and arc length). This practice automatically satisfies equation (1) inasmuch as it increases the energy input, E, thereby decreasing the total number of cracks, Y. (Refer to Appendix.)

It should be noted here that a simpler correlation between each of the individual welding variables and other cracking criteria was not found. This is explained by the very complex role of the variables in determining the thermal conditions, the weld profile, composition and microstructure, all of which are combined in the cracking phenomenon.

According to Pellini's strain theory (Ref. 5), the last stage of solidification (just above the solidus temperature) consists of dendrites separated by liquid films. If stress is imposed on the solidifying metal, high unit strains that develop in the inter-

Table 2—Welding Experimental Data[a]

Exp. no.	Weld speed cm/min	Current, A	Weld energy, joules/cm	Total no. of cracks
1	2	20	9,200	29
2	↓	24	14,040	9
3		35	21,000	6
4	3	24	8,760	23
5		35	13,030	22
6		50	19,000	11
7		65	23,400	15
8		80	30,400	9
9	5	24	6,340	16
10		35	12,075	26
11		40	8,160	18
12		45	9,180	31
13		50	10,200	12
14	8	24	3,780	21
15		35	5,380	26
16		50	8,000	22
17		65	9,978	23
18		76	13,680	55
19	10	35	3,150	14

(a) Each datum point represents two or more experiments.

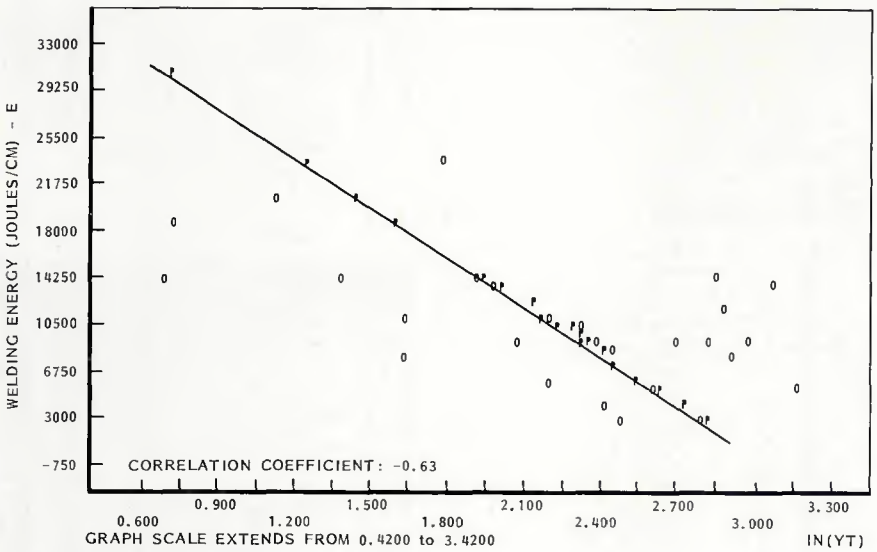

Fig. 4 — Computer plot of observed (O) and predicted (P) values of welding energy vs. IN (total number of cracks) in the weld (YT)

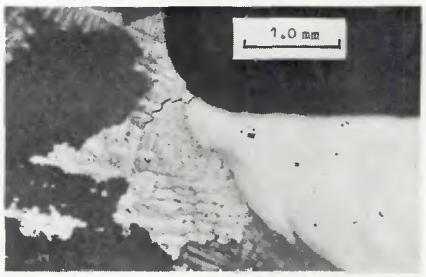

Fig. 5 — Typical grain boundary crack in the HAZ of IN-713C welded hardware

dendritic regions may exceed the local rupture strain to result in cracking. In other words, the rate of straining predominates in determining whether cracking will occur.

Based on the terminology developed by Hemsworth et al. (Ref. 6), weld cracking in alloy 713C seems to fall in the liquation class inasmuch as it was observed to be associated with grain boundary liquation at the HAZ. Figure 5 shows a typical grain boundary crack of alloy 713C hardware. It is possible, however, that a subsolidus ductility dip (Ref. 6) would account for the cracking just as well, since a ductility dip was observed in several Ni-base superalloys (Ref. 7). An attempt was not made here to determine the mechanism by which the weld cracking occurs in alloy 713C. However, Pellini's strain theory as applied to weld cracking (Ref. 8), even though originally developed for grain boundary liquation, would still hold true and is thus adopted to explain the observations outlined above.

Thermal stresses are generated in welding as a result of steep temperature gradients associated with rapid heating and solidification rates, by virtue of the weld undergoing expansion in a "cold" matrix. Expansion can be further inhibited by mechanical clamping, thereby increasing both the stress level and the rate of straining. The plates used in this study were not clamped, but were free to move in all directions. Thus, the main source of straining was that of the metal away from the weld. A thermal induced elastic stress can be described by the following expression:

$$\sigma = E(T) \cdot \alpha(T) \cdot \Delta T$$

where E is Young's modulus and α is the expansion coefficient. The major contribution to the stress level is ΔT, but the latter changes with time, hence, determines the strain rate as follows:

$$\dot{\epsilon} = \frac{\partial \epsilon}{\partial t} = \frac{d}{dt}\left(\frac{\Delta L}{L}\right) = \frac{d}{dt}\left(\frac{\alpha(t) \cdot L \cdot \Delta T(t)}{L}\right) = \frac{d}{dt}\left[\alpha(t)\Delta T(t)\right]$$

Since the temperature difference, ΔT, dictates both the strain level and the rate of straining, it is a logical step to analyze the temperature distribution in arc welding. Figure 6 (Ref. 9) shows temperature distribution curves for different times (in seconds) elapsed since the electrode

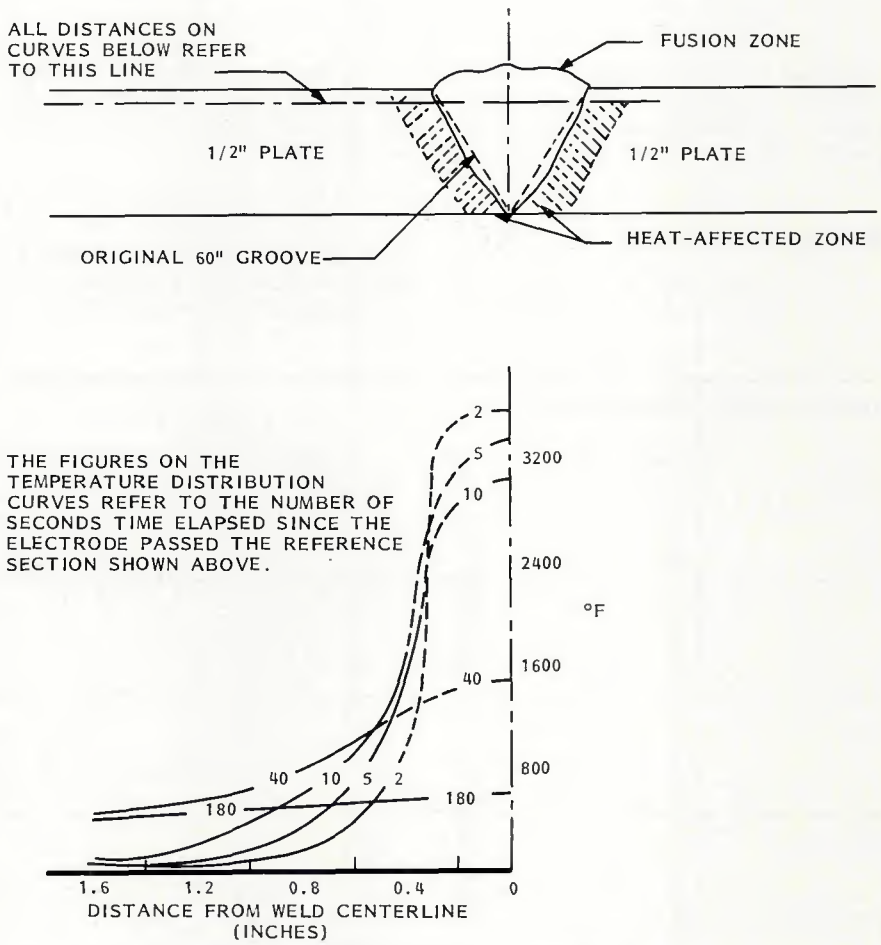

Fig. 6 — Temperature distribution in the neighborhood of an electric arc weld (From Nippes and Savage, Ref. 9)

passed in the reference section. The data were generated with arc welding of ½ in. (12.7 mm) mild steel plate using energy input of 70,000 joules in.$^{-1}$ (27,559 joules cm^{-1}). It should be noted that the maximum temperature and cooling rate at any point vary inversely with its distance from the center line (Ref. 9), but the shape of the temperature curves will strongly depend on the energy input, on the dimensions of the plate being welded (i.e., its width and thickness), and on the thermal conductivity of the alloy.

The significance of these factors cannot be appreciated unless a specific case is studied. In the experiments we conducted, the energy input ranged from 3,150 to 30,400 joules cm^{-1} (Table 2); this resulted in weld widths ranging from 2 to 15 mm (.079 to 0.59 in.), respectively. Assuming symmetry of temperature distribution curves about the center, only half the plate width counts when thermal stresses are considered. Recalling that the width of each plate was 35 mm (1.38 in.), it is interesting to note that the ratio (in percentage) of the bead width over half the plate width ranged from 11.5 to 85.5%.

This geometrical factor cannot be neglected; in fact, the heat transfer boundary conditions cannot be approximated by those for a semi-infinite plate as is normally done in welding of large parts. Furthermore, a considerable "end effect" exists which increases with energy input. Thus, it can be assumed that on cooling the rate of change of the temperature distribution curves increases with energy input. In addition, since the puddle size as well as the peak temperature increase with the energy input, solidification time becomes longer; consequently, more time is allowed for the temperature gradient to drop off. Hence, the rate of straining and the maximum stress imposed on the solidifying metal at the time the liquid film stage is reached are smaller for larger energy inputs. This evidently accounts for the observed reduction in total number of cracks at increased levels of energy input.

Although conflicting evidence is found in published works, it is a common experience that weld microstructure associated with higher energy input favors cracking susceptibility, due to factors such as weld pool profile, grain size, microsegregation, dendrite arm spacing, center line macrosegregation, etc. (Ref. 10). In addition, energy input level controls the degree of dissolution and reprecipitation of γ' phase, which contributes to straining due to volume changes and also controls grain boundary film formation as a result of elevated temperature chemical reactions of γ' with the solid solution matrix, γ. However, the effect of weld energy input parameters on cracking as a result of its effect on weld and HAZ microstructure is believed to be of secondary importance in the specific set of conditions of the present study.

The more pronounced effect of welding speed on cracking than that of welding current is attributed to the rate at which the energy input is transferred to the work-piece. As a result of different welding speeds, a given energy input per unit length can be delivered in different time periods. For instance, 12,000 joules per cm is obtainable by welding at a speed of 20 mm/min or at a speed of 8 cm/min., using a current of 20 or 80 amperes (A), respectively. However, in the first set of parameters, it is accomplished within 30 s whereas, in the second set, only within 7.5 s. Accordingly, when a lower speed is employed, temperature gradients experienced on heating are shallower. This results in shallower temperature gradients on cooling also which, in turn, reduces the rate of straining imposed on the solidifying weld.

Finally, it should be noted that equation (2), due to its empirical nature, is bound to be affected by factors such as thermal conductivity, chemistry, microstructure, high temperature ductility, and external mechanical constraints. Nevertheless, qualitative deductions may be made for similar alloys and geometrical dimensions. For different applications, preheating and/or post-heating are worth trying and normally will result in increased yields (Ref. 11).

Acknowledgments

This work was supported by the Israel Ministry of Trade and Commerce. One of the authors, A. Koren, wishes to thank Ms. Anne Jagodnik for typing the manuscript.

References

1. Ikawa, H.; Shin, S.; and Makao, Y. 1971. *Weldability of nickel base resisting superalloy—main cause of weld crackings in heat affected zone on IN-713C.* Japan: Osaka University.

2. Ikawa, Hiroshi. 1971. Study on weld crackings in Ni-base superalloy, Inconel 713C. Trans. Japan Welding Society, vol. 2, no. 2.

3. Duvall, D. S., and Doyle, J. R. 1973 (April). Repair on turbine blades and vanes. Paper presented at Gas Turbine and Products Show of ASME, Washington, D. C.

4. Koren, A.; Roman, H.; Weisshaus, I.; and Kaufman, A. 1980. The effect of weld energy input parameters on the crack sensitivity of alloy IN-713C. *Physical metallurgy of metal joining.* New York: AIME.

5. Pellini, W. S. 1952 (November). Strain theory of hot tearing. *The foundry* 125.

6. Hemsworth, B.; Boniszewski, T.; and Eaton, N. F. 1969. Classification and definition of high temperature welding cracks in alloys. *Metal Construction and British Welding Journal,* Feb. (S).

7. Yamaguchi, S.; Kobayashi, H.; Matsumiya, T.; and Hayami, S. 1979 (May). Effect of minor elements on hot workability of nickel-base superalloys. *Metal technology.*

8. Apblett, W. R., and Pellini, W. S. 1954. Factors which influence weld hot cracking. *Welding Journal* 33(2):83-s to 90-s.

9. Nippes, E. F., and Savage, W. F. 1949. Development of specimens simulating weld HAZ's. *Welding Journal* 28(11):534-s to 546-s.

10. Davies, G. J., and Garland, J. G. 1975. Solidification structure and properties of fusion welds. *International metallurgical reviews,* vol. 20.

11. King, R. W.; Hatala, R. W.; and Hauser, H. A. 1970 (November). Welding of superalloy turbine hardware. *Metals Eng. Quarterly.*

12. Essers, W. G., and Walter, R. 1981. Heat transfer and penetration mechanisms with GMA and plasma-GMA welding. *Welding Journal* 60(2):37-s to 42-s.

Appendix: Energy Input Calculation

The energy input per unit length in arc welding is known to have the following form:

$$E = \frac{V \cdot I \cdot 60}{S}$$

where: E = electrical energy in joules/cm; V = D.C. weld potential in volts, I = D.C. weld current in amperes, and S = welding speed in cm/in.

The heat transfer efficiency (namely, the fraction of heat input to work-piece over the total energy input), although expected to be much less than 100%, was dropped from the computations because of the assumption that it was constant over the entire range of experiments (Ref. 12).